Monte Carlo study of skin optical clearing to enhance light penetration in the tissue

Alexey N. Bashkatov[1] , Valery V. Tuchin[1], Elina A. Genina[1], Mikhail M. Stolnitz[1], Dmitry M. Zhestkov[1], Gregory B. Altshuler[2], Ilya V. Yaroslavsky[2]

[1] Institute of Optics and Biophotonics, Department of Optics and Biomedical Physics of Saratov State University, Saratov, Russia
[2] Palomar Medical Technologies, Inc, Burlington, USA

ABSTRACT

Result of Monte Carlo simulations of skin optical clearing is presented. The model calculations were carried out with the aim of studying of spectral response of skin under immersion liquids action and calculation of enhancement of light penetration depth. In summary, we have shown that: 1) application of glucose, propylene glycol and glycerol produced significant decreasing of light scattering in different skin layers; 2) maximal clearing effect will be obtained in case of optical clearing of skin dermis, however, absorbed light fraction in skin dermis changed insignificantly, independently from clearing agent and place it administration; 4) in contrast to it, the light absorbed fraction in skin adipose layer increased significantly in case of optical clearing of skin dermis. It is very important because it can be used for development of optical methods of obesity treatment.

Keywords: optical clearing, skin, optical properties, glucose, glycerol, propylene glycol

1. INTRODUCTION

Recent technological advancements in the photonics industry have led to a resurgence of interest in optical imaging technologies and real progress toward the development of non-invasive clinical functional imaging systems. Over the last decade, non-invasive or minimally invasive spectroscopy and imaging techniques have witnessed widespread exciting applications in biomedical diagnostics, for example, optical coherence tomography (OCT)[1,2], visible and near-infrared elastic-scattering spectroscopy[3,4], fluorescent[1,3,5] and polarization spectroscopy[6,7]. Spectroscopic techniques are capable of deep-imaging of tissues that could provide information of blood oxygenation[8] and detect cutaneous, brain and breast tumors[9], whereas confocal microscopy[10], OCT[2,11] and multi-photon excitation imaging[10,12] have been used to show cellular and sub-cellular details of superficial living tissues. Spectroscopic and OCT techniques are applicable for blood glucose monitoring with diabetic patients[13-15]. Besides diagnostic applications, optical methods are widely used in modern medicine, for example, for photodynamic therapy[16,17] and for laser surgery of different diseases[18,19]. Interest in using optical methods for physiological-condition monitoring and cancer diagnostics and therapies has been increased due to their simplicity, safety, low cost, contrast and resolution features in contrast to conventional X-ray computed tomography and ultrasound imaging[9].

The main limitations of the majority of the imaging techniques, including OCT and near-infrared (NIR) spectroscopy deal with the strong light scattering in superficial tissues[9,20-23], which cause decrease of spatial resolution, low contrast, and small penetration depth. Solution of the problem, i.e. reducing light scattering, and thus improving image quality and precision of spectroscopic information, can be connected with control of tissue optical properties. It is well-known that the major source of scattering in tissues and cell structures is the refractive index mismatch between cell organelles, like mitochondria, and cytoplasm, extracellular media and tissue structural components such as collagen and elastin fibers[9,11,24,25]. The tissue scattering properties can be significantly changed due to action of osmotically active immersion liquids[9,23,26-37]. Similar results have been obtained for optical clearing of whole blood[22,38-40]. Administration of the immersion liquid having a refractive index higher than that of tissue interstitial fluid induces a partial replacement of the interstitial fluids by immersion substance and hence, matching of refractive indices of tissue scatterers and the interstitial fluid. Osmotic activity of the immersion agents may cause tissue dehydration that also equalizes refractive indices within

bash@optics.sgu.ru

Complex Dynamics and Fluctuations in Biomedical Photonics IV, edited by Valery V. Tuchin,
Proc. of SPIE Vol. 6436, 64360Z, (2007) · 1605-7422/07/$18 · doi: 10.1117/12.716874

a tissue. Matching, correspondingly, causes the decrease of scattering. As osmotic immersion liquids, aqueous solutions of glucose and mannitol, propylene glycol, glycerol and other biocompatible chemicals are used.

Goal of this study is Monte Carlo modeling of spectral response of the skin under immersion liquids action and calculation of enhancement of light penetration depth.

2. SKIN STRUCTURE AND OPTICAL MODEL

Skin presents a complex heterogeneous tissue where blood and pigment content are spatially distributed variably in depth[41-43]. Skin consists of three main layers from the surface: epidermis (100 μm thick, the blood-free layer), dermis (1-2 mm thick, vascularised layer), and subcutaneous adipose tissue (from 1 to 6 mm thick, in dependence of the body site). Typically, the optical properties of the layers are characterized by absorption μ_a and scattering μ_s coefficients, which are equal to the average number of absorption and scattering events per unit path length of photon travel in the tissue and the anisotropy factor *g*, which represents the average cosine of the scattering angles.

The randomly inhomogeneous distribution of blood and various chromophores and pigments in skin produces variations of average optical properties of skin layers. Nonetheless, it is possible to define the areas in skin, where the gradient of skin cells structure, chromophores or blood amounts changing with a depth equals roughly zero[41]. This allows subdividing these layers into sublayers regarding the physiological nature, physical and optical properties of their cells, and pigment content. The epidermis can be subdivided into two sublayers: non-living and living epidermis. Non-living epidermis or stratum corneum (about 20 μm thick) consists of only dead squamous cells, which are highly keratinized with high lipid and protein content, and has a relatively low water content[41,42]. Living epidermis (100 μm thick) contains most of the skin pigmentation, mainly melanin, which is produced in the melanocytes[44]. Large melanin particles such as melanosomes (> 300 nm in diameter) exhibit mainly forward scattering. Whereas, melanin dust, whose particles are small (< 30 nm in diameter), has the isotropy in the scattering profile, and optical properties of the melanin particles (30-300 nm in diameter) may be predicted by the Mie theory.

Dermis is a vascularised layer and the main absorbers in the visible spectral range are the blood hemoglobin, carotene and bilirubin. In the IR spectral range, absorption properties of skin dermis are determined by absorption of water. Following the distribution of blood vessels[43] skin dermis can be subdivided into four layers: the papillary dermis (150 μm thick), the upper blood net plexus (100 μm thick), the reticular dermis (1-2 mm thick) and the deep blood net plexus (100 μm thick). The scattering properties of the dermal layers are mainly defined by the fibrous structure of the tissue, where collagen fibrils are packed in collagen bundles and have lamellae structure. Light scatters on both single fibrils and scattering centers, which are formed by the interlacement of the collagen fibrils and bundles. It is important, that the average scattering properties of the skin are defined by the scattering properties of the reticular dermis because of relatively big thickness of the layer (up to 2 mm) and comparable scattering coefficients of the epidermis and the reticular dermis. Absorption of hemoglobin and water of skin dermis and lipids of skin epidermis defines the absorption properties of the whole skin.

In accordance with the structural and morphological properties of skin, in this study, we presented planar seven-layer optical model of skin (see, Fig. 1). The particular layers included in the model are the stratum corneum, the living epidermis, the basal layer of epidermis, the three layers of dermis (such as the reticular dermis with upper vessel plexus, the dermis and the lower vessel plexus) and the subcutaneous adipose tissue layer. Thickness of the layers as well as blood and water content, refractive indices of the layers and mean vessel diameters are presented in Table 1.

Table 1. The parameters of skin layers used in the simulation[35,36,45,47]

Skin layers	Thickness, μm	Refractive index	Water content (%, vol/vol)	Blood content (%, vol/vol)	Scattering coefficient at 577 nm (bloodless), cm^{-1}	Mean vessel diameter, μm
Stratum corneum	20	1.5	0	0	300	-
Living epidermis	100	1.4	60	0	300	-
Basal layer	15	1.4	60	0	300	-
Reticular dermis & upper vessel	200	1.38	75	1.7	120	6

plexus						
Dermis	1500	1.35	75	1.4	120	15
Lower vessel plexus	100	1.38	75	1.7	120	6
Subcutaneous adipose tissue	3000	1.44	5	0	130	-

In the visible and NIR spectral ranges, the absorption coefficient of each layer includes contributions from the three basic chromophores: blood, melanin and water. The corresponding expression[45]:

$$\mu a_k = B_k C_k \mu a_{blood}(\lambda) + (1 - B_k - W_k)\mu a_{bg} + M_k \mu a_{mel}(\lambda) + W_k \mu a_{water}(\lambda), \quad (1)$$

where $k = 1,\ldots,7$ is the layer number, B_k and W_k are the volume fractions of blood and water in the layer, factor M_k is a unity for the melanin containing layers including living epidermis, and basal layer and M_k is zero for the other layers, C_k is the correction factor, μa_{blood}, μa_{mel}, μa_{water} and μa_{bg} are the absorption coefficients of blood, melanin, water and background tissue absorption, respectively. The later absorption coefficient is suggested to be wavelength independent and equal to 0.15 cm^{-1}. The correction factors are the number from zero through unity, taking into account the fact that blood is confined to the vessels rather than being distributed homogeneously in the tissue bulk[45]. Actually, if the vessels thick enough the light cannot penetrate to its inner part and, therefore, the interior of the vessel does not work as an absorber. If this is the case, the correction factor is appreciably smaller than a unity. Conversely, for very thin vessels the correction factor is close to a unity. It follows from this discussion that correction factor depends on the mean vessel diameter and the blood absorption coefficient at the particular wavelength. To evaluate these factors the numeric data from[47] have been approximated by the relation: $C_k = \dfrac{1}{1 + a\left(0.5\mu a_{blood} d_k^{\text{vessels}}\right)^b}$, where d_k^{vessels} is blood vessels diameter, cm. In case of collimated illumination of the vessels the coefficients a and b have values $a = 1.007$ and $b = 1.228$. In the case of diffuse illumination of the vessels the coefficients a and b have values $a = 1.482$ and $b = 1.151$. Optical (the absorption and the scattering) properties of blood have been calculated by us earlier[48]. In this study, we use typical values 0.4 for the hematocrit and 0.8 for the oxygen saturation, the later being the average value for the venous (0.7) and arterial (0.9) blood. The absorption spectrum of water in the visible and NIR may be found in Refs. 49-51.

The total scattering coefficient can be defined as[45]:

$$\mu s_k(\lambda) = B_k C_k \mu s_{blood}(\lambda) + (1 - B_k)\mu s T_k(\lambda). \quad (2)$$

The total scattering coefficient of the bloodless tissue, $\mu s T_k$, falls with the increase in the wavelength. In this study, the following relation has been used[45]:

$$\mu s T_k(\lambda) = \mu s 0_k \left(\frac{577\,\text{nm}}{\lambda}\right), \quad (3)$$

where $\mu s 0_k$ are the scattering coefficients at the reference wavelength 577 nm listed in Table 1.

The expression for the anisotropy of scattering may be constructed to include the contribution from blood[45]:

$$g_k(\lambda) = \frac{B_k C_k \mu s_{blood}(\lambda) g_{blood} + (1 - B_k)\mu s T_k(\lambda) gT(\lambda)}{\mu s_k(\lambda)} \quad (4)$$

where $gT(\lambda)$ is the anisotropy factor of the bloodless tissue and

$$gT(\lambda) = 0.7645 + 0.2355\left[1 - \exp\left(-\frac{\lambda - 500\,\text{nm}}{729.1\,\text{nm}}\right)\right]. \quad (5)$$

Melanin is confined entirely to the epidermis with its total concentration depending on the skin type. In the context of our seven-layer model there are two layers containing melanin: the living epidermis and basal layers. The partitioning of

melanin between the two layers depends on the skin type as well. For light skin, melanin is confined mainly to the basal layer, whereas for dark skin the distribution of melanin in the epidermis is somewhat more homogeneous. For skin type III (in accordance with Fitzpatrick classification) investigated in this study, we use the following relationship, which describes the melanin absorption coefficient:

$$\mu a_{\text{mel}}(\lambda) = A \exp\left(-\frac{\lambda - 800\,\text{nm}}{182\,\text{nm}}\right), \tag{6}$$

where parameter A is relation optical density of pigmented layer (living epidermis or basal layer) to their thickness. In accordance with data presented in Ref. 45 the parameter is equal to 0.87 cm^{-1} for living epidermis and 13.5 cm^{-1} for basal layer.

The optical properties (the absorption and scattering coefficients and anisotropy factor) of the skin layers have been calculated in accordance with the presented model and the result presented in Figs. 2-4.

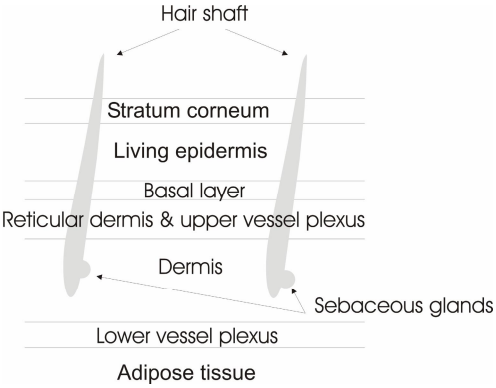

Fig. 1. The seven-layer optical model of skin

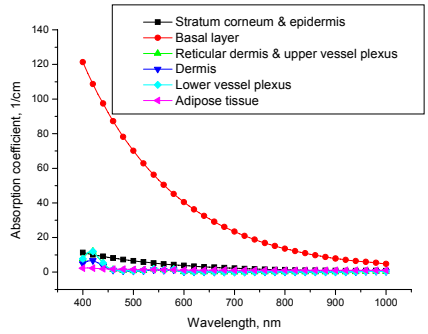

Fig. 2. The absorption spectra of different skin layers calculated in accordance with presented optical model

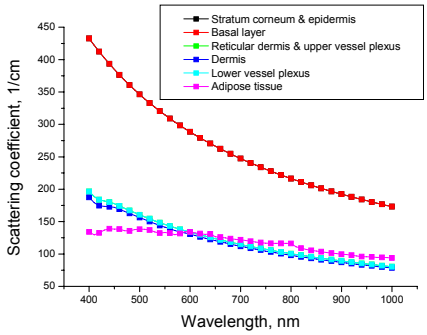

Fig. 3. The scattering spectra of different skin layers calculated in accordance with presented optical model

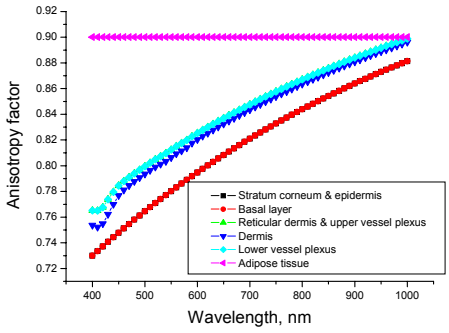

Fig. 4. The wavelength dependence of anisotropy factor of different skin layers calculated in accordance with presented optical model

3. MATERIALS AND METHODS

In this study, we used Monte Carlo algorithm developed by L. Wang and presented in Ref. 52. The stochastic numerical MC method is widely used to model optical radiation propagation in complex randomly inhomogeneous highly scattering and absorbing media such as biological tissues[9,26,35,36]. Basic MC modeling of an individual photon packets trajectory consists of the sequence of the elementary simulations[52]: photon path length generation, scattering and

absorption events, reflection or/and refraction on the medium boundaries. The initial and final states of the photons are entirely determined by the source and detector geometry. For simplicity, the incident light is assumed to be a pencil beam and the photons packets are launched normally to the tissue surface. The specular reflection from the air–tissue surface is taking into account in the simulations. At the scattering site a new photon packet direction is determined according to the Henyey–Greenstein scattering phase function: $f_{\mathrm{HG}}(\theta)=\frac{1}{4\pi}\frac{1-g^2}{\left(1+g^2-2g\cos\theta\right)^{3/2}}$, where θ is the polar scattering angle. The distribution over the azimuthal scattering angle was assumed as uniform. MC technique requires values of absorption and scattering coefficients and anisotropy factor of each skin layer, its thickness and refractive indices and the required data have been presented in Figs. 2-4 and Table 1.

For modeling of skin optical clearing we calculated the scattering properties (see Figs. 2-4) using Mie theory. The theory required knowledge of refractive indices of skin scatterers and interstitial fluid and sizes of the skin scatterers. In the calculations, for approximation of scattering properties of stratum corneum, living epidermis and basal layers we used spherical particles and for approximation of scattering properties of dermal layers we used cylindrical particles. Since the function of distribution of skin scatterers and packing factor are unknown now, we used for the calculations monodisperse, so-called Mie-equivalent, particles. In this case, for upper layers, scattering coefficients can be calculated as $\mu_s(\lambda)=\frac{3}{4}\frac{\varphi}{\pi a^3}\pi a^2 Q_s(a,n_s,n_I)F(\lambda)$, where a is scatterers radius (spheres), $Q_s(a,n_s,n_I)$ is scattering efficacy factor, $F(\lambda)$ is packing factor, n_s is refractive index of scatters and n_I is refractive index of interstitial fluid, i.e. surrounding medium, and φ is volume fraction of scatterers for each layer. For dermal layers the scattering coefficient can be calculated with the similar equation $\mu_s(\lambda)=\frac{\varphi}{\pi a^2}2aQ_s(a,n_s,n_I)F(\lambda)$, but in this case, a is the scatterers radius (cylinders), and $Q_s(a,n_s,n_I)$ will be calculated for cylindrical particles, too. In this study, we calculated the effective scattering size and packing factor for each wavelength by minimization of the target function

$$\mathrm{TF}(a(\lambda),F(\lambda))=\left(\mu_s^{\mathrm{model}}-\mu_s^{Mie}\right)^2+\left(g^{\mathrm{model}}-g^{Mie}\right)^2. \quad (7)$$

Here μ_s^{model} is data presented in Fig. 3 and g^{model} is data presented in Fig. 4 for each layer. μ_s^{Mie} is scattering coefficient calculated for each layer with formulas presented above. g^{Mie} is anisotropy factor calculated to find effective scatterers size using Mie theory.

For investigating the influence of clearing agents on the optical parameters of skin (the diffuse reflectance, total transmittance and the light absorbed fraction), the skin interstitial fluid (water) has been changed to clearing agents in series for different skin layers. Sizes of effective skin scatterers, packing factor and refractive index of skin scatterers are constant during all calculations. Skin layers thickness is constant, too. As clearing agents the glycerol (refractive index 1.47), the propylene glycol (refractive index 1.43), and 40%-aqueous solution of glucose (refractive index 1.39) have been used.

4. RESULTS AND DISCUSSION

Figures 5 and 6 demonstrated optical clearing of skin after immersion of the skin by glucose solution. Fig. 5 shows reflectance spectra calculated in the framework of the presented model in the spectral range from 400 to 1000 nm. From the figure it is seen that immersion of upper skin layers (the stratum corneum, living epidermis, basal layer and reticular dermis with upper vessel plexus) changed the skin reflectance insignificantly. However, optical clearing of dermis produced significant decreasing of skin reflectance. Similar result has been observed for skin transmittance. Figure 6 shows transmittance spectra of skin calculated in the framework of the presented model in the spectral range from 400 to 1000 nm at immersion of different skin layers by glucose solution. From the figure it is seen that immersion of upper skin layers (the stratum corneum, living epidermis, basal layer and reticular dermis with upper vessel plexus) changed the skin transmittance insignificantly. However, optical clearing of skin dermis produced significant increasing of skin

transmittance. It is connected with decreasing of the skin scattering properties due to the partial replacement of skin dermis interstitial fluid by glucose solution. The significant decreasing of skin reflectance and corresponding increasing of skin transmittance are connected with bigger thickness of skin dermis in comparison with thickness of the other skin layers.

In the spectral range 400-900 nm, the form of the presented spectra is defined by the absorption bands of blood of the upper and deep blood net plexus of skin with maxima at 415, 540 and 575 nm, and the spectral dependence of the scattering properties of the skin dermis. Absorption of water in this spectral range is negligible[49]. The main scatterers of the dermal layer are collagen fibrils packed in collagen bundles and scattering centers, which are formed by the interlacement of the collagen fibrils and bundles. In the spectral range from 900 to 1000 nm the form of the presented spectra is defined by the absorption band of water with maximum at 975 nm[50,51] and the spectral dependence of the scattering properties of the skin dermis. The influence of skin melanin which localized in upper skin layers connected with decreasing both reflectance and transmittance of skin, especially in the short-wavelength spectral range.

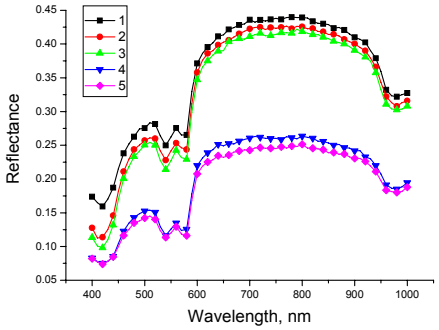

Fig. 5. The reflectance spectra of skin before and after the skin immersion by glucose solution

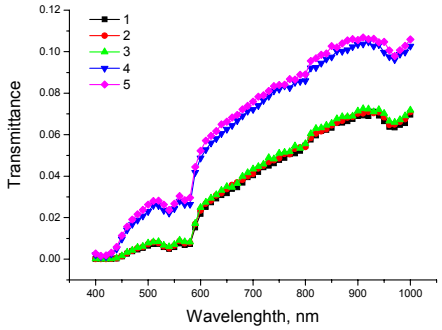

Fig. 6. The transmittance spectra of skin before and after the skin immersion by glucose solution

1- without clearing; 2 – Stratum corneum, living epidermis & basal layer immersed;
3 - Stratum corneum, living epidermis, basal layer & reticular dermis immersed;
4 - Stratum corneum, living epidermis, basal layer, reticular dermis & dermis immersed;
5 - Stratum corneum, living epidermis, basal layer, reticular dermis, dermis & lower vessel plexus immersed

Figures 7-9 demonstrated evolution of light absorbed fraction in different skin layers at immersion of the layers by glucose solution. Fig. 7 shows wavelength dependence of light absorbed fraction in upper skin layers at immersion of the layers by glucose solution. From the figure it is seen that immersion of upper skin layers (the stratum corneum, living epidermis, basal layer and reticular dermis with upper vessel plexus) changed of the light absorbed fraction insignificantly. However, optical clearing of dermis produced significant decreasing of the light absorbed fraction. It is connected with increase of light penetration depth into skin and corresponding decreasing of backscattering flux from lower skin layers. Opposite result has been obtained for skin adipose layer (see, Fig. 9). From the figure it is seen that optical clearing of skin dermis produced significant increasing of light penetration depth into skin and corresponding increase of the light absorbed fraction in subcutaneous adipose tissue. It is a very interesting result obtained for skin dermis (see, Fig. 8). From the figure it is seen that light absorbed fraction is not changed independently from optical clearing of any skin layers. That can be explained by the fact that fluence rate in the layer is formed by backscattering flux from subcutaneous adipose tissue.

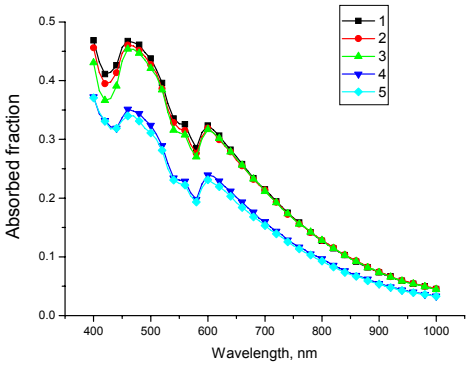

Fig. 7. The absorbed fraction of light in upper (the stratum corneum, epidermis & basal) layers of skin before and after the skin immersion by glucose solution

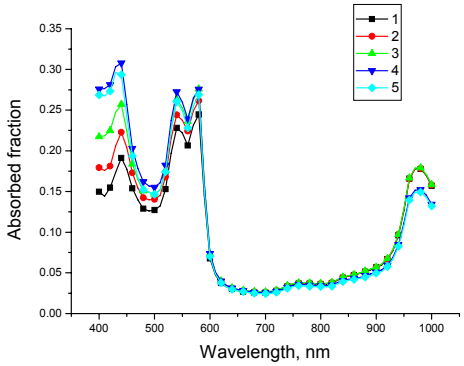

Fig. 8. The absorbed fraction of light in skin dermis before and after the skin immersion by glucose solution

1- without clearing; 2 – Stratum corneum, living epidermis & basal layer immersed;
3 - Stratum corneum, living epidermis, basal layer & reticular dermis immersed;
4 - Stratum corneum, living epidermis, basal layer, reticular dermis & dermis immersed;
5 - Stratum corneum, living epidermis, basal layer, reticular dermis, dermis & lower vessel plexus immersed

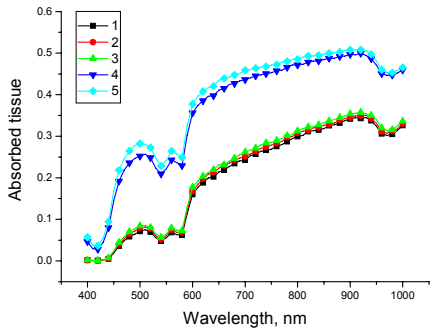

Fig. 9. The absorbed fraction of light in skin adipose layer before and after the skin immersion by glucose solution

1- without clearing; 2 – Stratum corneum, living epidermis & basal layer immersed;
3 - Stratum corneum, living epidermis, basal layer & reticular dermis immersed;
4 - Stratum corneum, living epidermis, basal layer, reticular dermis & dermis immersed;
5 - Stratum corneum, living epidermis, basal layer, reticular dermis, dermis & lower vessel plexus immersed

Figures 10-14 presented the results of computer modeling of skin optical clearing by propylene glycol. From these figures it is seen that the obtained results are very close to the results presented in figures 5-9, which is connected with skin optical clearing by glucose solution. That can be explained by differences between value of refractive index of collagen (the main structural component of biological tissues including skin) and refractive indices of glucose solution and propylene glycol. Mean value of refractive index of collagen is 1.41, value of refractive index of glucose solution is 1.39, and value of refractive index of propylene glycol is 1.43. In both cases the differences between refractive indices of tissue scatterers and surrounding medium is 0.02, and thus the scattering efficacy has to change in the similar manner.

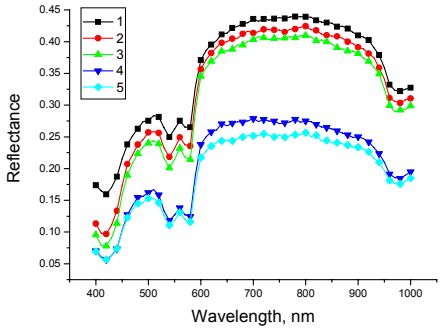

Fig. 10. The reflectance spectra of skin before and after the skin immersion by propylene glycol

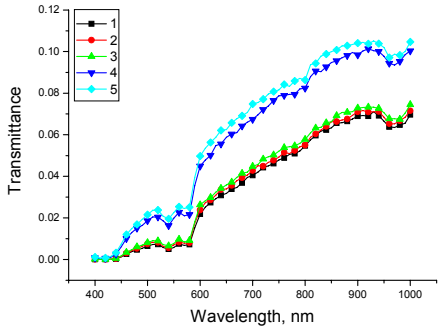

Fig. 11. The transmittance spectra of skin before and after the skin immersion by propylene glycol

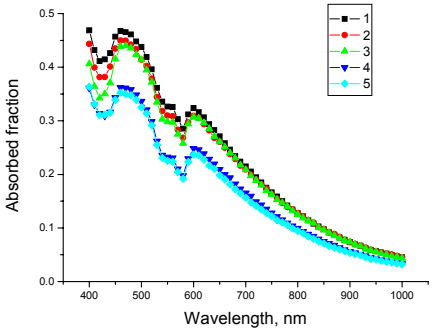

Fig. 12. The absorbed fraction of light in upper (the stratum corneum, epidermis & basal) layers of skin before and after the skin immersion by propylene glycol

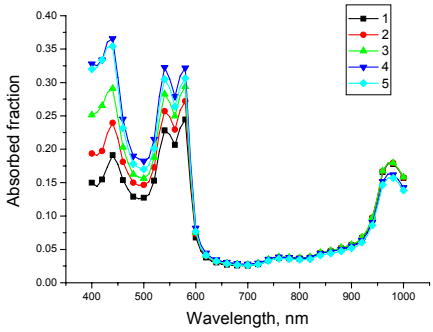

Fig. 13. The absorbed fraction of light in skin dermis before and after the skin immersion by propylene glycol

1- without clearing; 2 – Stratum corneum, living epidermis & basal layer cleared;
3 - Stratum corneum, living epidermis, basal layer & reticular dermis cleared;
4 - Stratum corneum, living epidermis, basal layer, reticular dermis & dermis cleared;
5 - Stratum corneum, living epidermis, basal layer, reticular dermis, dermis & lower vessel plexus cleared

Figures 15-19 presented the results of computer modeling of skin optical clearing by glycerol. From these figures it is seen that the obtained results are different in comparison from the results obtained for skin optical clearing by glucose solution and propylene glycol. From figures 15 and 16 it is seen that glycerol produced is significantly smaller than propylene glycol and glucose solution decreasing of skin reflectance and increasing of skin transmittance. That can be explained by differences between value of refractive index of collagen (the main structural component of biological tissues including skin) and refractive indices of glycerol. Mean value of refractive index of collagen is 1.41, value of refractive index of glycerol is 1.47. In this case replacement of water (interstitial fluid in normal state) by glycerol produced only insignificant reducing of skin scattering. Figures 17-19 show wavelength dependence of light absorbed fraction in different skin layers at immersion the layers by glycerol. Fig. 17 shows light absorbed fraction in the upper skin layers at immersion of the layers by glycerol. From the figure it is seen that immersion of any skin layers changed the light absorbed fraction in the upper skin layers insignificantly. The similar result has been observed for skin dermis, too (see, Fig. 18).

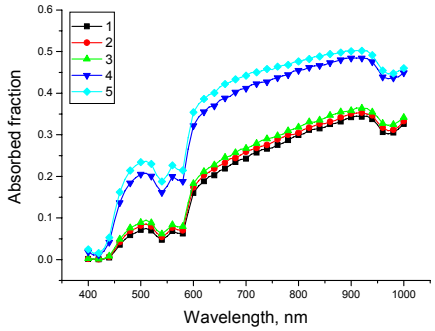

Fig. 14. The absorbed fraction of light in skin adipose layer before and after the skin immersion by propylene glycol

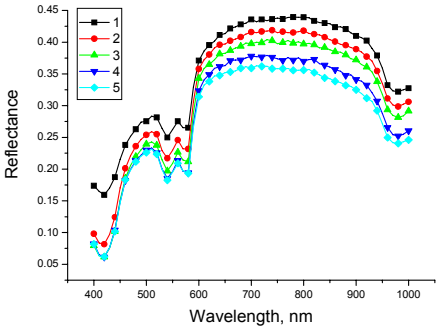

Fig. 15. The reflectance spectra of skin before and after the skin immersion by glycerol

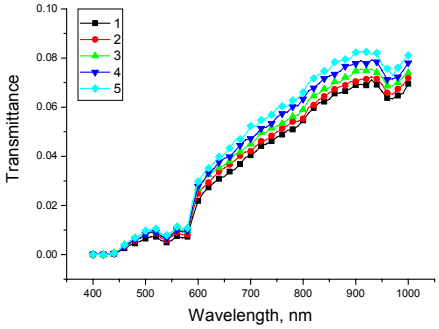

Fig. 16. The transmittance spectra of skin before and after the skin immersion by glycerol

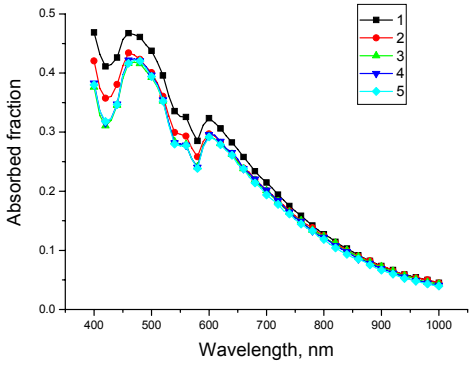

Fig. 17. The absorbed fraction of light in upper (the stratum corneum, epidermis & basal) layers of skin before and after the skin immersion by glycerol

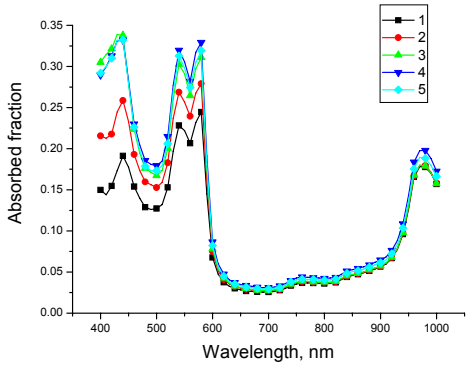

Fig. 18. The absorbed fraction of light in skin dermis before and after the skin immersion by glycerol

1- without clearing; 2 – Stratum corneum, living epidermis & basal layer immersed;
3 - Stratum corneum, living epidermis, basal layer & reticular dermis immersed;
4 - Stratum corneum, living epidermis, basal layer, reticular dermis & dermis immersed;
5 - Stratum corneum, living epidermis, basal layer, reticular dermis, dermis & lower vessel plexus immersed

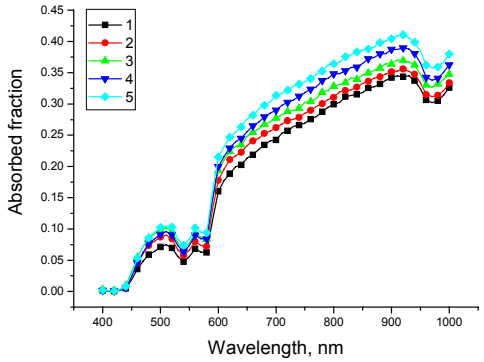

Fig. 19. The absorbed fraction of light in skin adipose layer before and after the skin immersion by glycerol

1- without clearing; 2 – Stratum corneum, living epidermis & basal layer immersed;
3 - Stratum corneum, living epidermis, basal layer & reticular dermis immersed;
4 - Stratum corneum, living epidermis, basal layer, reticular dermis & dermis immersed;
5 - Stratum corneum, living epidermis, basal layer, reticular dermis, dermis & lower vessel plexus immersed

5. CONCLUSION

In this paper we presented results of Monte Carlo simulations of skin optical clearing. The model calculations were carried out with the aim of studying of spectral response of skin under immersion liquids action and calculation of enhancement of light penetration depth. In summary, we have shown that: 1) application of glucose, propylene glycol and glycerol produced significant decreasing of light scattering in different skin layers. 2) maximal clearing effect will be obtained in case of optical clearing of skin dermis. 3) at the same time, absorbed light fraction in skin dermis changed insignificantly, independently from clearing agent and place it administration. 4) in contrast to it, the light absorbed fraction in skin adipose layer increased significantly in case of optical clearing of skin dermis. It is very important because it can be used for development of optical methods of obesity treatment.

ACKNOWLEDGEMENTS

The research described in this publication has been made possible, in part, by grants PG05-006-2 and REC-006 of U.S. Civilian Research and Development Foundation for the Independent States of the Former Soviet Union (CRDF) and the Russian Ministry of Science and Education, grant of the Russian Federal Agency of Education Russian Federation 1.4.06, and grant of RFBR No. 06-02-16740-a. The authors thank Dr. S.V. Eremina (Department of English and Intercultural Communication of Saratov State University) for the help in manuscript translation to English.

REFERENCES

1. N. Kollias, G.N. Stamatas, "Optical non-invasive approaches to diagnosis of skin diseases," *Oct. JID Symposium Proc.,* 7, 64-75 (2002).
2. A.F. Fercher, W. Drexler, C.K. Hitzenberger, T. Lasser, "Optical coherence tomography – principles and applications," *Rep. Prog. Phys.,* 66, 239-303 (2003).
3. I.J. Bigio, J.R. Mourant, "Ultraviolet and visible spectroscopies for tissue diagnostics: fluorescence spectroscopy and elastic-scattering spectroscopy," *Phys. Med. Biol.,* 42, 803-814 (1997).
4. P. Thueler, I. Charvet, F. Bevilacqua, M. Ghislain, G. Ory, P. Marquet, P. Meda, B. Vermeulen, C. Depeursinge, "*In vivo* endoscopic tissue diagnostics based on spectroscopic absorption, scattering, and phase function properties," *J. Biomed. Opt.,* 8, 495-503 (2003).
5. S. Andersson-Engels, C. Klinteberg, K. Svanberg, S. Svanberg, "In vivo fluorescence imaging for tissue diagnostics," *Phys. Med. Biol.,* 42, 815-824 (1997).
6. S.L. Jacques, J.C. Ramella-Roman, K. Lee, "Imaging skin pathology with polarized light," *J. Biomed. Opt.,* 7, 329-340 (2002).

7. A.N. Yaroslavsky, V. Neel, R.R. Anderson, "Demarcation of nonmelanoma skin cancer margins in thick excisions using multispectral polarized light imaging," *J. Invest. Dermatol.,* 121, 259-266 (2003).
8. H. Liu, D.A. Boas, Y. Zhang, A.G. Yodh, B. Chance, "Determination of optical properties and blood oxygenation in tissue using continuous NIR light," *Phys. Med. Biol.,* 40, 1983-1993 (1995).
9. V.V. Tuchin, *Tissue Optics: Light Scattering Methods and Instruments for Medical Diagnosis*, SPIE Press, TT38, Bellingham, USA, 2000.
10. B.R. Masters, P.T.C. So, "Confocal microscopy and multi-photon excitation microscopy of human skin in vivo," *Optics Express,* 8**,** 2-10 (2001).
11. V.V. Tuchin, "Coherent optical techniques for the analysis of tissue structure and dynamics," *J. Biomed. Opt.,* 4, 106-124 (1999).
12. B.R. Masters, P.T.C. So, E. Gratton, "Optical biopsy on in vivo human skin: multi-photon excitation microscopy," *Lasers Med. Sci.,* 13, 196-203 (1998).
13. R.J. McNichols, G.L. Cote, "Optical glucose sensing in biological fluids: an overview," *J. Biomed. Opt.,* 5, 5-16 (2000).
14. K. Xu, Q. Li, Z. Lu, J. Jiang, "Fundamental study on non-invasive blood glucose sensing," *J. X-Ray Science and Technology,* 10, 187-197 (2002).
15. K.V. Larin, M. Motamedi, T.V. Ashitkov, R.O. Esenaliev, "Specificity of noninvasive blood glucose sensing using optical coherence tomography technique: a pilot study," *Phys. Med. Biol.,* 48, 1371-1390 (2003).
16. V.V. Tuchin, E.A. Genina, A.N. Bashkatov, G.V. Simonenko, O.D. Odoevskaya, G.B. Altshuler, "A pilot study of ICG laser therapy of *acne vulgaris*: photodynamic and photothermolysis treatment," *Lasers Surg. Med.,* 33, 296-310 (2003).
17. E.A. Genina, A.N. Bashkatov, G.V. Simonenko, O.D. Odoevskaya, V.V. Tuchin, G.B. Altshuler, "Low-intensity indocyanine-green laser phototherapy of acne vulgaris: pilot study," *J. Biomed. Opt.,* 9, 828-834 (2004).
18. T.S. Dietlein, P.C. Jacobi, G.K. Krieglstein, "Erbium:YAG laser trabecular ablation (LTA) in the surgical treatment of glaucoma," *Lasers Surg. Med.,* 23, 104-110 (1998).
19. B.A. Buscher, T.O. McMeekin, D. Goodwin, "Treatment of leg telangiectasia by using a long-pulse dye laser at 595 nm with and without dynamic cooling device," *Lasers Surg. Med.,* 27, 171-175 (2000).
20. D.A. Boas, "A fundamental limitation of linearized algorithms for diffuse optical tomography," *Optics Express,* 1, 404-413 (1997).
21. C.L. Smithpeter, A.K. Dunn, A.J. Welch, R. Richards-Kortum, "Penetration depth limits of *in vivo* confocal reflectance imaging," *Appl. Opt.,* 37**,** 2749-2754 (1998).
22. M. Brezinski, K. Saunders, C. Jesser, X. Li, J. Fujimoto, "Index matching to improve optical coherence tomography imaging through blood," *Circulation,* 103, 1999-2003 (2001).
23. R.K. Wang, X. Xu, V.V. Tuchin, J.B. Elder, "Concurrent enhancement of imaging depth and contrast for optical coherence tomography by hyperosmotic agents," *J. Opt. Soc. Am. B*, 18, 948-953 (2001).
24. J.M. Schmitt, G. Kumar, "Optical scattering properties of soft tissue: a discrete particle model," *Appl. Opt.,* 37, 2788-2797 (1998).
25. R.K. Wang, "Modelling optical properties of soft tissue by fractal distribution of scatters," *J. Mod. Opt.,* 47, 103-120, (2000).
26. V.V. Tuchin, I.L. Maksimova, D.A. Zimnyakov, I.L. Kon, A.H. Mavlutov, A.A. Mishin, "Light propagation in tissues with controlled optical properties," *J. Biomed. Opt.,* 2, 401-417 (1997).
27. A.N. Bashkatov, V.V. Tuchin, E.A. Genina, Yu.P. Sinichkin, N.A. Lakodina, V.I. Kochubey, "The human sclera dynamic spectra: in vitro and in vivo measurements," *Proc. SPIE,* 3591, 311-319, (1999).
28. A.N. Bashkatov, E.A. Genina, V.I. Kochubey, N.A. Lakodina, V.V. Tuchin, "Osmotical liquid diffusion within sclera," *Proc. SPIE,* 3908**,** 266-276, (2000).
29. A.N. Bashkatov, E.A. Genina, I.V. Korovina, V.I. Kochubey, Yu.P. Sinichkin, V.V. Tuchin, "*In vivo* and *in vitro* study of control of rat skin optical properties by acting of osmotical liquid," *Proc. SPIE,* 4224**,** 300-311 (2000).
30. A.N. Bashkatov, E.A. Genina, I.V. Korovina, Yu.P. Sinichkin, O.V. Novikova, V.V. Tuchin, "*In vivo* and *in vitro* study of control of rat skin optical properties by action of 40%-glucose solution," *Proc. SPIE,* 4241**,** 223-230 (2001).
31. A.N. Bashkatov, E.A. Genina, Yu.P. Sinichkin, V.V. Tuchin, "The influence of glycerol on the transport of light in the skin," *Proc. SPIE,* 4623**,** 144-152 (2002).

32. A.N. Bashkatov, E.A. Genina, V.V. Tuchin, "Optical immersion as a tool for tissue scattering properties control," in *Perspectives in Engineering Optics*, K. Singh and V. K. Rastogi, editors. Anita Publications, New Delhi, India. 313-334 (2002).
33. A.N. Bashkatov, E.A. Genina, Yu.P. Sinichkin, V.I. Kochubei, N.A. Lakodina, V.V. Tuchin, "Estimation of the glucose diffusion coefficient in human eye sclera," *Biophysics*, 48(2), 292-296 (2003).
34. A.N. Bashkatov, E.A. Genina, Yu.P. Sinichkin, V.I. Kochubey, N.A. Lakodina, V.V. Tuchin, "Glucose and mannitol diffusion in human *dura mater," Biophys. J.,* 85, 3310-3318 (2003).
35. I.V. Meglinskii, A.N. Bashkatov, E.A. Genina, D.Yu. Churmakov, V.V. Tuchin, "Study of the possibility of increasing the probing depth by the method of reflection confocal microscopy upon immersion clearing of near-surface human skin layers," *Quantum Electronics,* 32, 875-882 (2002).
36. I.V. Meglinski, A.N. Bashkatov, E.A. Genina, D.Y. Churmakov, V.V. Tuchin, "The enhancement of confocal images of tissues at bulk optical immersion," *Laser Physics,* 13, 65-69 (2003).
37. E.A. Genina, A.N. Bashkatov, V.I. Kochubey, V.V. Tuchin, "Optical clearing of human dura mater," *Optics and Spectroscopy*, 98(3), 470-476 (2005).
38. V.V. Tuchin, X. Xu, R.K. Wang, "Dynamic optical coherence tomography in studies of optical clearing, sedimentation, and aggregation of immersed blood," *Appl. Opt.,* 41, 258-271 (2002).
39. X. Xu, R.K. Wang, J.B. Elder, V.V. Tuchin, "Effect of dextran-induced changes in refractive index and aggregation on optical properties of whole blood," *Phys. Med. Biol.,* 48, 1205-1221 (2003).
40. V.V. Tuchin, D.M. Zhestkov, A.N. Bashkatov, E.A. Genina, "Theoretical study of immersion optical clearing of blood in vessels at local hemolysis," *Optics Express,* 12, 2966-2971 (2004).
41. K.S. Stenn, "The skin," in *Cell and Tissue Biology* ed by L Weiss (Baltimore: Urban & Shwarzenberg), 541-572 (1988.)
42. G.F. Odland, "Structure of the skin,*"* in *Physiology, Biochemistry, and Molecular Biology of the Skin*, 1, ed by L A Goldsmith, Oxford University Press, Oxford (1991).
43. T.J. Ryan, *Cutaneous Circulation* (*In* Physiology, Biochemistry, and Molecular Biology of the Skin, 1, ed by L A Goldsmith, Oxford University Press, Oxford), (1991).
44. M.R. Chedekel, "Photophysics and photochemistry of melanin," in *Melanin: Its Role in Human Photoprotection* eds. L Zeise, M R Chedekel and T B Fitzpatrick (Overland Park: Valdenmar) 11-22 (1995).
45. G. Altshuler, M. Smirnov, I. Yaroslavsky, "Lattice of optical islets: a novel treatment modality in photomedicine," *Journal of Physics D: Applied Physics*, 38, 2732-2747 (2005).
46. A.N. Bashkatov, E.A. Genina, V.I. Kochubey, V.V. Tuchin, "Optical properties of human skin, subcutaneous and mucous tissues in the wavelength range from 400 to 2000 nm," *Journal of Physics D: Applied Physics*, 38, 2543-2555 (2005).
47. W. Verkruysse, G.W. Lucassen, J.F. de Boer, D.J. Smithies, J.S. Nelson, M.J.C. van Gemert, "Modelling light distributions of homogeneous versus discrete absorbers in light irradiated turbid media," *Phys. Med. Biol.*, 42, 51-65, (1997).
48. A.N. Bashkatov, D.M. Zhestkov, E.A. Genina, V.V. Tuchin, "Immersion clearing of human blood in the visible and near-infrared spectral regions," *Optics and Spectroscopy*, 98(4), 638-646 (2005).
49. R.C. Smith, K.S. Baker, "Optical properties of the clearest natural waters (200-800nm)," *Appl. Opt.,* 20, 177-184 (1981).
50. L. Kou, D. Labrie, P. Chylek, "Refractive indices of water and ice in the 0.65-2.5μm spectral range," *Appl. Opt.,* 32, 3531-3540 (1993).
51. K.F. Palmer, D. Williams, "Optical properties of water in the near infrared," *J. Opt. Soc. Am.,* 64, 1107-1110 (1974).
52. L. Wang, S.L. Jacques, L. Zheng, "MCML – Monte Carlo modeling of light transport in multi-layered tissues," *Computer Methods and Programs in Biomedicine*, 47, 131-146 (1995).